

3—15

Surface Evolution Based on Wave Propagation and Its Application to Topology-Adaptive 3-D Modeling

Kenji Hara *

Department of Electronics Technology
Fukuoka Industrial Technology Center

Hongbin Zha[†]

Tsutomu Hasegawa[†]
Department of Intelligent Systems
Kyushu University

Abstract

Deformable surfaces have been successfully used for modeling 3-D objects. However, they have not been able to model multi-object scenes or objects with holes. In the paper, we propose a new method of modeling objects of arbitrary topology by using a surface evolution approach based on wavefront propagation. Differing from level set modeling methods, we do not require repeated distance transformations and increased dimensions, and hence the method is computationally efficient. The method has been applied in several experiments using range data, and the results are reported in the paper.

1 Introduction

Recently, a lot of methods have been proposed for automatic modeling of 3-D free-form objects from multi-view range images ([1]). The resulting models, however, are usually still large data sets comprising great amounts of unorganized 3-D points. To build a model-base easy to use for model retrieval, we have to transform the data further into some structural, compact but global descriptions.

The framework of optimization based on deformable surfaces was successfully used in the past for such descriptions ([2], [3]). Deformable surfaces have the ability to generate smooth close-surfaces on the basis of energy minimization. However, deformable surfaces have a serious drawback in modeling multi-object scenes or objects of arbitrary topology such as those with holes. One method for overcoming this problem is to apply a level set method ([4], [5]) to interfaces propagating with curvature-dependent speeds. However, the methods are computationally inefficient since they require repeated distance transformations and increased dimensions.

In the paper, we propose a new method of modeling multi-object scenes or objects of arbitrary topology efficiently by a surface evolution approach based on wave propagation. At first, we build a narrow-band stopping region by dilating every data point.

*Address: 3-6-1 Norimatsu, Yahatanishi-ku, Kitakyushu 807-0831 Japan. E-mail: hara@itc.pref.fukuoka.jp

[†]Address: 6-10-1 Hakozaki, Higashi-ku, Fukuoka 812-8581 Japan. E-mail: {zha,hasegawa}@is.kyushu-u.ac.jp

We set an initial region whose boundary is a single surface covering the 3-D data on the whole close-surface(CS) of the object. Then, we let the boundary evolve by repeated erosions with a ball structuring element, which is based on Huygens' principle for wavefront propagation. Here, the ball has the size increasing monotonously as the curvature of the surface increases. Therefore, the surface shrinks and splits while keeping smoothness and avoiding self-intersection. Moreover, the radius of the ball structuring element is defined as zero if its center lies in the stopping region, and thus every surface point stops moving near the border of the stopping region. However, if the width of the stopping region is too large, the resultant surface would be still different topologically from the object surface. On the contrary, if it is too small, there remain holes due to the data missing. Thus, it is necessary to design an algorithm for finding the appropriate widths.

First, after the above surface fitting to the stopping region with a comparatively large width, the stopping region is narrowed. After that, this fitting-and-narrowing cycle is repeated until the number of the data points lying in the neighborhood of the surface is almost equal to the total number of data points. Note that the former would be smaller than the latter if the width of the stopping region is so large that it makes the model and the object surfaces topologically different.

After the above rough estimation, for model refinement, we extract a quadrangular mesh from the resultant surface, and then perform precise fitting to the original CS data on the basis of an energy minimization. The method has been applied in several experiments using synthetic image and real one, and the results are reported in the paper.

2 Surface Evolution Based on Wave Propagation

We introduce a surface evolution approach based on the integration of Huygens' principle and curvature-dependent flow. While this approach does not always yield the solutions satisfying differential equations, we can obtain the surfaces evolving while developing no self-intersections and preserving smoothness. Differing from the level set approach

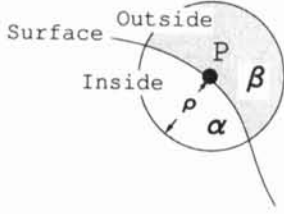


Figure 1: Amount of convexity

([4], [5]), our approach can trace the evolving surface at small computational costs without increasing dimensions and repeatedly searching for the closest points.

Here, we let the close-surface smoothly contract and split by repeated erosions with a variable-size ball structuring element. The radius $r = r(\mathbf{p}, t)$ of the ball centering any point $\mathbf{p} = (x, y, z)^T$ on the evolving surface at the time t is defined as

$$r(\mathbf{p}, t) = r_0 + \epsilon K, \quad (1)$$

where r_0 and ϵ are positive constants. With $\epsilon = 0$, the limit of this evolution produces the Huygens' principle for wavefront propagation. $K = K(\mathbf{p}, t)$ is the amount of convexity of the surface at \mathbf{p} , and it is introduced instead of noise-sensitive 3-D curvatures. Therefore, the second term ϵK can be regarded as a smoothing term. K is defined as the volume rate of the region outside the surface in the neighborhood of \mathbf{p} , and thus it is defined as

$$K = -\frac{\alpha - \beta}{\alpha + \beta}, \quad (2)$$

where $\alpha = \alpha(\mathbf{p}, t)$ and $\beta = \beta(\mathbf{p}, t)$ are the numbers of inside cells and outside ones, respectively, within the distance ρ from \mathbf{p} (Fig.1).

3 Topology-Adaptive Modeling by Surface Evolution Approach

In the section, we describe in detail two procedures involved in our topology-adaptive modeling method.

3.1 Initial Estimation

At first, we set a region whose boundary is a single close-surface covering the given whole CS data. Then, we let this boundary smoothly contract and split by the surface evolution approach stated earlier. Now, modifying eq.(1), we define the size $r = r(\mathbf{p}, t)$ of the structuring element as

$$r(\mathbf{p}, t) = \begin{cases} \max(r_0 + \epsilon K, 0) & \mathbf{p} \text{ is outside } S \\ 0 & \text{otherwise,} \end{cases} \quad (3)$$

where S is called the stopping region, and any surface point lying in this region attains zero speed. We define a stopping region S for the whole CS data by

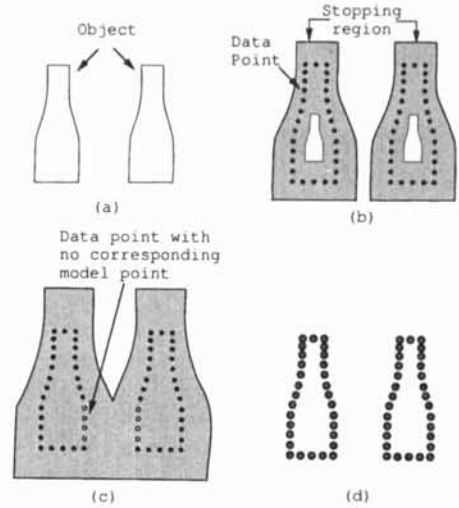


Figure 2: Influence of the width of stopping region

expanding every data point into a ball with radius δ , where δ can be roughly computed by the width of the stopping region. Note that, as shown in Fig.2(b), we suppose that there exists some δ such that the surface lying outside S is topologically equivalent to the object surface.

According to eq.(1), the evolving boundary contracts with time and then stops at points lying outside S . As a result, we can obtain a model surface topologically equivalent to the object surface. However, if the value of δ is too large, the surface lying outside S would be still different topologically from the object surface (Fig.2(c)). On the contrary, if the value of δ is too small, there remain holes due to the data missing (Fig.2(d)). Thus, it is necessary to design an algorithm for finding the optimal value of δ .

We first select a comparatively large value as the initial value of δ , and then track the boundary evolving according to eq.(1). To judge whether the resulting model surface is topologically equivalent to the object surface, we introduce a detection rate

$$q = \frac{N_r}{N} \times 100(\%), \quad (4)$$

where N_r is the number of the data points having model points within the distance δ , and N the total number of the data points. Here, if q is smaller than a threshold th , δ is lowered since it is inferred that the current model is wrong in the topology. This process consisting of fitting to S and narrowing δ is iterated until q exceeds th . The above procedure for initial estimation is called first-stage in the paper.

3.2 Model Refinement

The model resulting from the above procedure provides a reasonable approximation to the object surface both in the shape and topology. This stage is employed mainly to enhance the accuracy of modeling by removing local irregularities resulting from

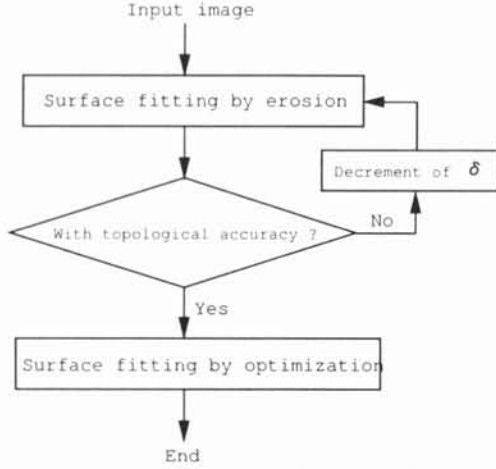


Figure 3: Outline of the algorithm.

the earlier evolution We extract an exterior quadrangular mesh from the cells composing this model, and switch to the popular regularization-based model approximation. Here, the energy function to be minimized can be expressed by

$$E_{point}(x) = E_{int}(x) + E_{est}(x), \quad (5)$$

where x is a set of vertices of the quadrangular mesh. The first term $E_{int}(x)$ corresponds to the smoothness constraint based on the springs imaginarily placed between neighboring vertices. The second term $E_{est}(x)$ is a data closeness term based on the springs placed between vertices and their nearest data points. The function (5) can be minimized fast by using the greedy algorithm ([8]). As a result, we can obtain the optimum quadrangular mesh fitted to 3-D data. The above procedure for model refinement is called final-stage in the paper.

The overall algorithm is outlined in Fig.3.

4 Experimental results

In this section, we present results of two experiments.

Fig.4(a) shows the CS data set synthesized from CAD data for a hexagon nut. At the beginning, we give a cubic close-surface covering the data, and set the width δ of the stopping region as 15. Next, we let this surface shrink until every surface point does not move, and then decrease δ by one. After repeating this process three times, we get the immediate result shown in Fig.4(b). Here, the detection rate q is 77.7%, which is too small, and thus the model in Fig.4(b) is regarded as being wrong topologically. After that, we lower δ further. The model obtained for $\delta = 8$ is shown in Fig.4(c). Here, q is 99.8% which is almost 100%, and therefore the first-stage is finished. The final model is shown in Fig.4(d).

Fig.5 shows the process of changing topology in each iteration by cross-sectional views. Fig.5(a)-(c)

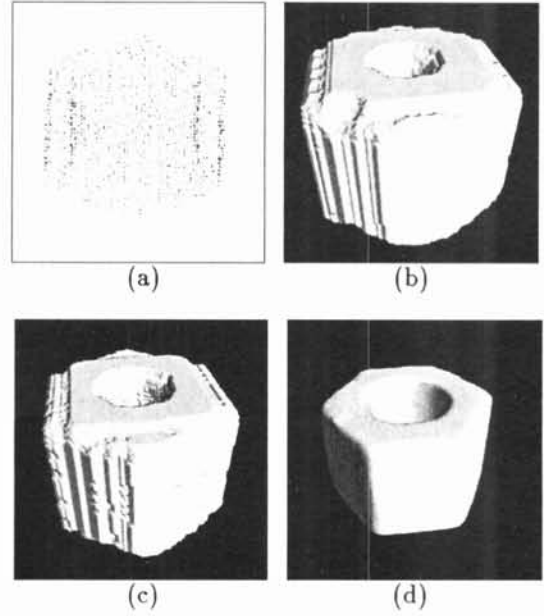


Figure 4: Experiment for the object with a hole

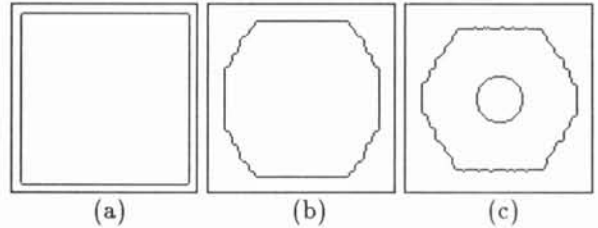


Figure 5: The process of topological changes

correspond to, respectively, $\delta = 15$ (the initial value), $\delta = 12$, and $\delta = 8$.

To compare our method with the existing topology-adaptive modeling method, intermediate results obtained using the fast level set approach called narrow-band algorithm are shown in Fig.6(a) and (b). These figures correspond to, respectively, Fig.4(b) and (c). As is evident here, there is not much difference between them.

Table 1 summarizes the surface evolution process in the first row indicating the figures in Fig.4 and Fig.6. The following rows correspond to, respectively, the widths of stopping region (δ), numbers of

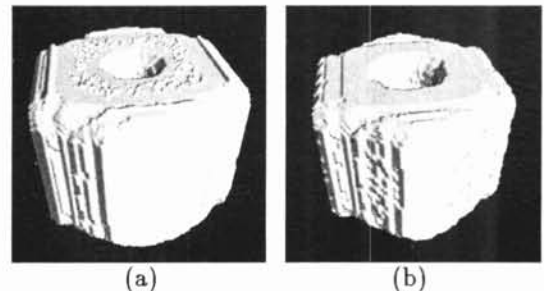


Figure 6: Experiment by level set modeling method

Table 1: Result summary of experiment

	Fig.4(b)	Fig.4(c)	Fig.4(d)	Fig.6(a)	Fig.6(b)
δ	12	8	-	12	8
N	38,075	37,843	8,744	38,309	36,370
T	199	254	756	2,822	3,495

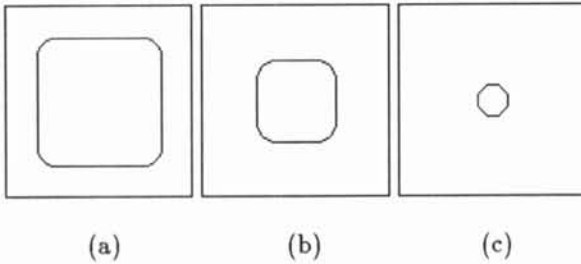


Figure 7: Process of surface evolving with smoothness

vertices (N), and used CPU times (T) in *sec.* on a Pentium II 300 *MHz* personal computer. Comparing the two CPU times corresponding to Fig.4(c) and Fig.6(b) in Table 1, our method is over ten times faster than the level set modeling method.

Fig.7(a)-(c) illustrate the cross-sections of the evolving surface when no stopping region is set. The smoothness of the surface is gradually increased in each step.

The second experiment aims to show the capacity of our method in modeling multi-object scene completely without a priori knowledge about the topology. The objects to be modeled are three statues including one with a hole shown in Fig.8(a). Fig.8(b) show the whole CS data. Fig.8(c)-(e) show the intermediate results. Here, the single close-surface splits into three ones while developing a hole in Fig.8(c) through (e). The final result is shown in Fig.8(f).

5 Conclusions

In the paper, we proposed a method of modeling a 3-D object of arbitrary topology by using a surface evolution approach based on wave propagation. Our algorithm has the advantage of being computationally efficient. It can also be implemented from a sparse data set without any knowledge about correspondences between data points and sensor viewpoints. In the future, we must analyze the proposed surface evolution method mathematically.

References

[1] H. Zha, K. Morooka, T. Hasegawa, "Active Modeling of 3-D Objects: Planning on the Next Best Pose (NBP) for Acquiring Range Images," *Proc. Int. Conf. Recent Advances in 3-D Digital Imaging and Modeling*, pp.68-75, 1997.

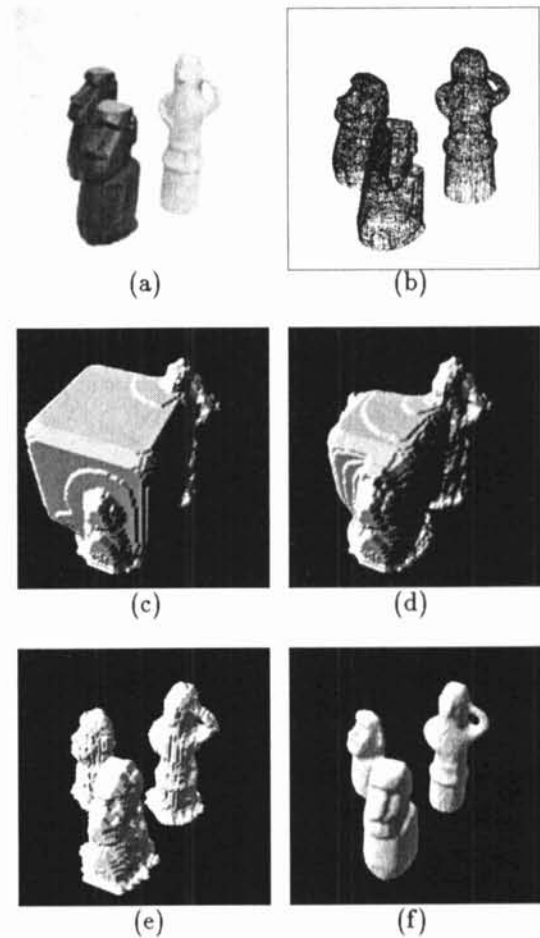


Figure 8: Experiment for multiple objects.

- [2] H. Delingette, M. Hebert, K. Ikeuchi, "Shape Representation and Image Segmentation Using Deformable Surfaces," *Proc. IEEE CVPR*, pp.467-472, 1991.
- [3] T. McInerney, D. Terzopoulos, "A Finite Element Model for 3D Shape Reconstruction and Nonrigid Motion Tracking," *Proc. ICCV*, pp.518-523, 1993.
- [4] S. Osher, J.A. Sethian, "Fronts Propagating with Curvature-Dependent Speed: Algorithms Based on Hamilton-Jacobi Formulation," *J. Comp. Phys.*, Vol.79, pp.12-49, 1988.
- [5] R. Malladi, J.A. Sethian, B.C. Vemuri, "Shape Modeling with Front Propagation: A Level Set Approach," *IEEE Trans. PAMI*, Vol.17, No.2, pp.158-175, 1995.
- [6] J.A. Sethian, "Curvature and the Evolution of Fronts," *Comm. in Math. Phys.*, Vol.101, pp.487-499, 1985.
- [7] D.L. Chopp, "Computing Minimal Surfaces via Level Set Curvature Flow," *J. Comp. Phys.*, Vol.106, pp.77-91, 1993.
- [8] D.J. Williams, M. Shah, "A Fast Algorithm for Active Contours," *Proc. ICCV*, pp.592-595, 1990.